FULL PAPER

WILEY-VCH

Parent, unsubstituted hemiporphycene: synthesis and properties

Jakub Ostapko,[a] Krzysztof Nawara,[a,b] Michał Kijak,[a] Joanna Buczyńska,[a] Barbara Leśniewska,[a] Mariusz Pietrzak,[a] Grażyna Orzanowska,[a] Jacek Waluk*[a,b]

Abstract: Among seven possible "nitrogen-in" constitutional isomers of porphyrin only one, porphycene, has been obtained so far as the free, unsubstituted form. We report the synthesis of another isomer, parent hemiporphycene (**HPc**), followed by thorough structural, spectral, photophysical, electrochemical, and theoretical studies. Most of the properties of **HPc** are intermediate between those of porphyrin and porphycene, as evidenced by the values of inner cavity dimensions, orbital energy splittings, absorption coefficients, magnetic circular dichroism parameters, NH stretching frequencies, fluorescence quantum yields, tautomerization rates, and redox potentials. The largest differences arise with respect to tautomerism, due to low symmetry of **HPc** and inequivalence of the four nitrogen atoms that define the inner cavity. Two *trans* tautomers are observed, separated in energy by ca. 1 kcal/mol. Tautomerization from the higher to lower energy form is detected in the lowest excited singlet state, occurring with a rate about four orders of magnitude lower than that observed for porphycene. Hemiporphycene emerges as a very good model for the investigation of inequivalent intramolecular hydrogen bonds present in one molecule: Two such bonds in **HPc** reveal unusual characteristics, and the bond strength results from the interplay between the N-N distance and the NHN angle.

now, only **Pr** and **Pc** have been known in their basic, unsubstituted form. A parent structure has also been obtained[10] for another isomer not belonging to the nitrogen-in family: "inverted"[11] or "confused"[12] porphyrin (**InPra**).
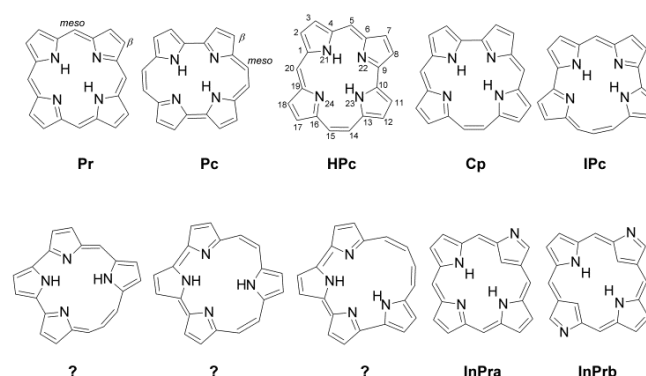
Scheme 1. Nitrogen-in and inverted/N-confused (**InPr**) porphyrin isomers. The structures labeled with a question mark have not been synthesized yet.

Introduction

The reason for the immense popularity of porphyrins can be found in the subtitle of the HANDBOOK OF PORPHYRIN SCIENCE: with Applications to Chemistry, Physics, Materials Science, Engineering, Biology and Medicine.[1] The research on porphyrins is constantly expanding in many diverse directions; one of them is based on the investigations of constitutional isomers of porphyrin (**Pr**). This field started in 1986 with the synthesis of porphycene (**Pc**).[2] Several years later, a theoretical paper discussed the electronic structure of all possible "nitrogen-in" isomers (Scheme 1), of which only porphycene was available at that time.[3] Three more isomers have been synthesized in the 90's: hemiporphycene (**HPc**),[4,5] corrphycene (**Cp**),[6,7] and isoporphycene (**IPc**).[8,9] However, unlike porphycene, they were all obtained in the form of substituted derivatives. Thus, until

[a]   J. Ostapko, Dr. K. Nawara, M. Kijak, Dr. J. Buczyńska, Dr. J. Leśniewska, Dr. M.Pietrzak, G. Orzanowska, Prof. J. Waluk
       Institute of Physical Chemistry, Polish Academy of Sciences,
       Kasprzaka 44, 01-224 Warsaw, Poland
   E-mail: waluk@ichf.edu.pl

[b]   Dr. K. Nawara, Prof. J. Waluk
       Faculty of Mathematics and Natural Sciences, College of Science,
       Cardinal Stefan Wyszyński University, Dewajtis 5, 01-815 Warsaw,
       Poland

       Supporting information for this article is given via a link at the end of the document.

Results and Discussion

Synthesis and structure. The first rational synthetic route leading to a hemiporphycene derivative has been provided by Vogel, Sessler, and coworkers in the synthesis of 2,3,7,8,11,12,17,18-octaethylhemiporphycene (**OEHPc**).[4] The proposed approach involves formation of an open-chain tetrapyrrolic α,ω-dialdehyde by MacDonald condensation of ethyl derivatives of 5,5'-diformyl-2,2'-bipyrrole and 5-carboxy-5'-formyl-2,2'-dipyrrylmethane, followed by McMurry olefination. Despite the great interest in the chemistry of porphyrin isomers, it has not been adopted to the synthesis of derivatives other than ethyl or etio and their metal complexes.[13-16] Other reports concerning formation of hemiporphycene derivatives also appeared, but, in all of these cases, hemiporphycene was obtained unexpectedly, as a product of free-base homoporphyrin ring contraction[5] or expansion of free-base corrole,[17,18] macrocycles known for the liability of their free-base forms. However, no general synthetic route employing ring expansion or contraction for hemiporphycene synthesis has been designed.

Here we present a rational approach leading to the formation of hemiporphycene (Scheme 2), which allowed us to obtain the parent, unsubstituted isomer dedicated to physicochemical characterization. The synthetic route relying on ring closure *via* McMurry reaction was examined, as the one successfully employed for the synthesis of porphycene,[2] octaethylhemiporphycene,[4] as well as tetramethyl-tetraethyl- and octaethylcorrphycenes.[6] The attempts to synthesize parent hemiporphycene via previously reported MacDonald

condensation route[4] failed due to instability of electron-rich unsubstituted pyrrolyldiene units. To overcome this problem, 1-*H* constitution of pyrrole rings in all the intermediate compounds was preserved. Moreover, *t*-butoxycarbonyl (*Boc*) protecting groups were introduced to di- and bipyrrole and oligopyrrole intermediates to provide the stability and to increase the solubility. The details describing syntheses of starting and intermediate materials are given in the Supporting Information (SI).

Boc-protected α,ω-dialdehyde **3** was easily obtained by BF₃·Et₂O assisted alkylation of 5-formyl-2,2'-bipyrrole **1** by a hydroxymethyl derivative of dipyrromethane **2**. Possible products of MacDonald self condensation of substrate **1** were formed in insignificant amounts. The protecting groups of dialdehyde **3** were removed by thermolysis, giving α,ω-dialdehyde **4** with good yield. The α,ω-dialdehyde **4** was used as a substrate in McMurry reaction. The conditions for this step were adopted from previous work.[4] The direct product of McMurry reaction, tetrapyrrolic macrocycle **5**, does not undergo rapid oxidation, therefore an oxidant has to be added. It was observed, according to TLC, that addition of DDQ or chloranil to the THF/ammonia solution of **5** leads to formation of many red-luminescent products, probably due to coupling of generated radicals. Fe^{3+} was found to be an inefficient oxidant under these conditions. Satisfying results were achieved by addition of Ag^+ salt to the solution of **5**. Silver salt provided complete oxidation and no formation of hemiporphycene-silver complexes was observed.

Similarly to the parent porphyrin and porphycene, hemiporphycene is poorly soluble in non-aromatic and non-chlorinated aromatic solvents, probably due to the stacking of unsubstituted aromatic rings, suggested by the crystal structure that reveals herringbone packing of molecules (Figure S20).
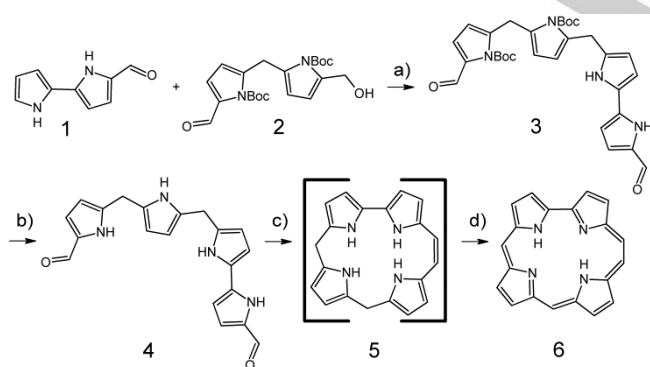

Scheme 2. Synthesis of hemiporphycene: a) BF₃·Et₂O/ DCM, THF, 76%; b) ethylene glycol, 150 ºC, 75%; c) TiCl₄, Zn, CuCl/ THF; d) AgNO₃, 6% (steps c and d).

Intermediates **1-3** were found to be stable under air atmosphere for at least one month. Decomposition of **4** was not observed over two weeks under the same conditions. The yield of hemiporphycene synthesis from α,ω-dialdehyde is lower than

in the case of its octaethylderivative (6% versus 20%,[4] respectively). The specific influence of ethyl substituents on cyclization and aromatization efficiency is unclear, however, the general tendency may be pointed out on the example of porphycene synthesis. When alkyl substituents are introduced to positions 4 and 4' of dialdehyde, the porphycene is formed with a higher yield than in the case of its parent structure. The presence of alkyl sbstituents in hemiporphycene precursor may have similar influence on its cyclization and aromatization yields.

¹H NMR spectra of **HPc** (**6**, Figure 1) were measured in THF-*d₈*. Signals assignment was performed basing on 2D NOESY spectrum (Figure S20). For comparison, the spectra of **Pc** (Figure S16) and **Pr** (Figure S17) were also measured under the same conditions. Due to low molecular symmetry, each proton in **HPc** has a different magnetic environment, which leads to a very rich spectrum in comparison with **Pr** and **Pc**. However, similarities to both, porphyrin[19] and porphycene[2] are obvious. Protons at C5 and C20 appear at low field (δ=9.98 and 10.32 ppm), similar to the corresponding *meso* position of porphyrin (δ=10.43 ppm). Doublets (J=12 Hz), assigned to protons at C14 and C15, appear at δ=9.86 and 9.76 ppm, respectively. The corresponding signal in porphycene appears as a singlet with δ=9.89. *β*-pyrrolic protons occupy the 9.6-9.0 ppm range of the spectrum. *β-H* at C7, C8, C17, and C18 are split into doublets (J=4.2 Hz), however *β-H* at C2, C3, C11 and C12 appear as doublet of doublets (J=4.2 Hz, J=1.8 Hz) due to the coupling with N-*H* (21, 23). The latter was confirmed by selective homodecoupling experiments (Figure S18). Absence of the smaller splitting of signals corresponding to *β-H* at C7, C8, C17, and C18 can be explained in terms of either existence of only one tautomer *trans1* or, more likely, tautomeric equilibrium *trans1-trans2* (Scheme 3), strongly shifted towards the more stable *trans1* tautomer. Nitrogen atoms 22 and 24 in *trans1* tautomer are not protonated and therefore the splitting of corresponding *β* protons is not observed.
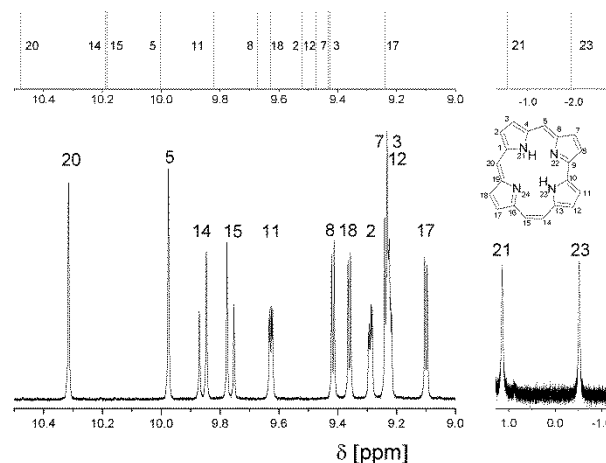
Figure 1. ¹H NMR spectrum of **HPc** in THF-*d₈* (293 K, 500 MHz) with experimental signals assignment. Top, calculated proton chemical shifts.

¹H NMR signals of the N-*H* protons appear at δ = 1.14 and -0.51 ppm. The chemical shifts of the N-*H* signals are located approximately halfway between the N-*H* signals of parent porphyrin (δ = -3.90) and porphycene (δ = 3.30 ppm). Contrary to the cases of **Pr** and **Pc**, the two intramolecular hydrogen bonds in **HPc** do not have the same strength, as illustrated by different chemical shifts and, moreover, by different responses of the N-*H* signals to changes in temperature (Figure S19). According to simulations of NMR spectra, the signals at 1.14 and -0.51 ppm can be assigned to protons attached to N21 and N23, respectively. This assignment is the same as that proposed for **OEHPc** by Vogel, Sessler, and coworkers,[4] based on the assumption that the stronger hydrogen bond corresponds to a smaller N-N distance. It is generally assumed that the proton chemical shift is a good measure of the strength of intramolecular hydrogen bond. However, the results presented below in the section devoted to vibrational structure suggest that **HPc** may represent an exception to this general rule, as the calculated N21H stretching frequency is higher (which indicates a weaker H-bond) than that of N23H, the latter corresponding to the longer N-N distance.

While the signals from the N-*H* protons are equally split in **HPc** and **OEHPc**, they are shifted to the lower field in the unsubstituted molecule, suggesting stronger intramolecular hydrogen bonds. This is in line with the calculated increase of the separation between H-bonded nitrogen atoms after substitution. This finding also explains why we did not observe the splitting of the N-*H* signals at low temperatures, whereas such effect, most likely due to freezing of *trans1-trans2* dynamic equilibrium, has been reported for **OEHPc**.[4]

The X-ray structure of **HPc** is presented in Figure S21. The crystals reveal structural disorder, which may be caused by different factors. In order to check the origin of structural disorder, we carried out the X-ray measurements at three different temperatures: 100, 173 and 293 K. The disorder was observed even at the lowest temperature, for which the presence of only one, most stable tautomeric form should be expected. Therefore, tautomerism does not seem to be the main reason for disorder.

Because of the disorder, the accurate determination of distances and angles, as well as comparison with theoretically optimized geometry was not possible. One can state, however, that the molecule is planar, as predicted by calculations.

The B3LYP/6-311++G(d,p) optimized geometries of **HPc**, **Pr**, and **Pc** were used as input for computation of the aromaticity indices. Very similar values of the HOMA (harmonic oscillator model of aromaticity) index[20] were obtained for the three compounds. For instance, when the classical 18π electron/18 bond system is taken as the main conjugation path, similar HOMA indices are obtained for all three isomers (0.94, 0.92, 0.90, and 0.92 for or **Pr**, **Pc**, *trans1*-**HPc** and *trans2*-**HPc**, respectively). When all 28 bonds are taken into account, one obtains the values of 0.68, 0.72, 0.70, and 0.71, respectively. Thus, no significant difference in aromaticity is revealed. This conclusion is supported by similar values of NICS (nucleus-independent chemical shift),[21] calculated at the center of the macrocyle for **Pr**, **Pc**, **HPc**(*trans1*), and **HPc**(*trans2*): -14.8, -13.0, -12.6, and -13.4, respectively.

Tautomerism. Hemiporphycene can assume six different tautomeric forms, two *trans* and four *cis* species (Scheme 3). In contrast to porphyrin and porphycene, no degeneracies are possible, because each nitrogen atom in **HPc** is chemically different. For solutions of **OEHPc** two forms have been observed.[22] They were assigned to *trans* tautomers. The difference in enthalpy was determined, using UV/VIS spectroscopy, as 0.65 kcal/mol, in agreement with the value estimated on the basis of NMR studies.[23]

We have optimized the structure and calculated the relative stabilities of all **HPc** tautomers. The results (Table 1) show that two lowest energy forms correspond to *trans* structures, separated by about 1 kcal/mol. Two pairs of *cis* species with each pair having similar energies are predicted. The energy difference between the *cis1/2* and *cis 3/4* pairs is much larger than that between *cis*1/2 and *trans*1/2, 15 vs 5 kcal-mol. Such behaviour is reminiscent of porphycene, for which two low-energy degenerate *trans* and *cis* tautomers are calculated very close in energy (2 kcal/mol), but the other *cis* tautomer lies much higher (30 kcal/mol).[24] It should be noted that the high energy *cis* form, though not populated in the ground electronic state, may be responsible for the radiationless depopulation of the excited states.[25] As discussed below, a similar mechanism may be postulated for **HPc**.
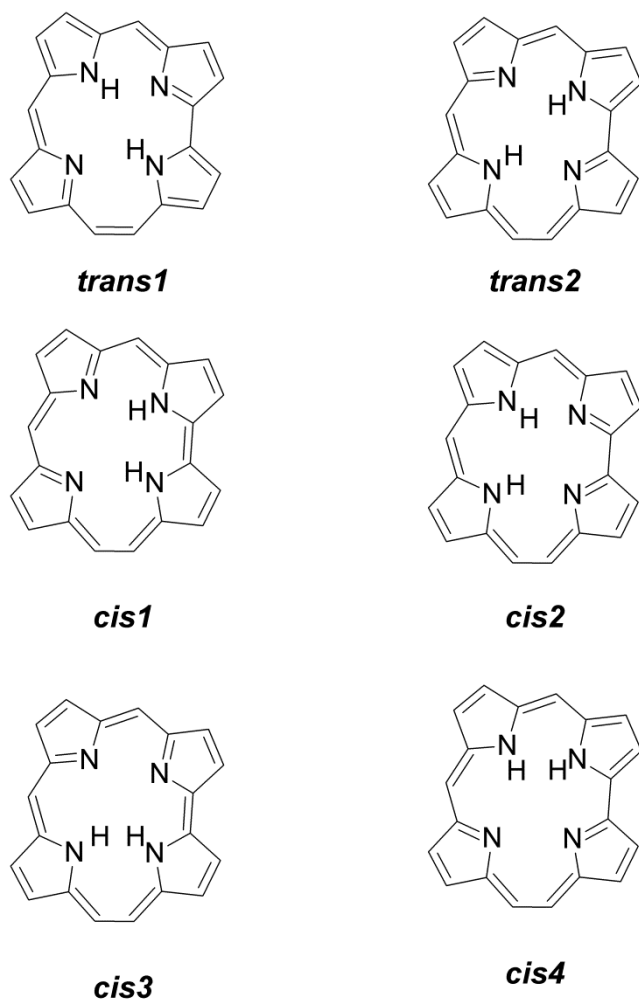
Scheme 3. Possible tautomeric forms of **HPc**.

Table 1. Calculated (B3LYP/6-311++G(d,p)) energies, dipole moments, and NH stretching frequencies of different tautomeric forms of **HPc**.

|	Relative energy [a] [kcal/mol]	Dipole moment [D]	NH1 str. freq. [cm^{-1}]	NH2 str. freq. [cm^{-1}]
Trans1	0.0 (0.0)	0.57	3312 (N23H)[b]	3366 (N21H)
Trans2	1.00 (0.88)	0.47	3302 (N22H)	3380 (N24H)
Cis1	4.50 (4.04)	1.73	2991 (N22H)	3104 (N23H)
Cis2	5.14 (4.49)	2.12	3035 (N21H)	3167 (N24H)
Cis3	19.39 (18.90)	1.94	3473 (N24H)	3614 (N23H)
Cis4	20.09 (19.57)	2.75	3454 (N21H)	3563 (N22H)

[a] In parentheses, values including zero-point vibrational energy. [b] atom numbering as in Scheme 1.

The reason for the large energy destabilization of specific *cis* forms seems to be the same in porphycene and hemiporphycene: it is the repulsion of the two inner hydrogen atoms that come very close to each other. For **HPc**, the calculated H-H distances are between 216 and 233 pm for both *trans*, *cis1*, and *cis2* forms, whereas for *cis3* and *cis4* these values are only 184 and 172 pm, respectively. It has been postulated[25] that high–lying *cis* forms of porphycene may become nonplanar in both ground and excited states, and that the ground electronic state may correspond to an open shell species. It remains to be investigated whether such behavior is also possible in hemiporphycene. Geometry optimization in S_0 predict nearly planar structure for all the tautomers. As could have been expected from the analysis of H-H distances, a deviation from planarity was obtained for *cis3* and *cis4*, but even here, the effect is not large: the four nitrogen atoms lie, within 1º, in a common plane.

The electronic absorption and fluorescence spectra of **HPc** recorded in nonpolar solvents (Figure 2) clearly demonstrate, similarly to the case of octaethylhemiporphycene, the presence of two species. Two bands are observed at the low energy side of the room temperature absorption spectrum, lying at 612 and 622 nm. Upon lowering the temperature, their relative intensities change and, finally, the lower energy band disappears. Upon heating the solution, the opposite behaviour is observed. The ratio of absorbances at 612 and 622 nm is thus a measure of the *trans1-trans2* equilibrium constant, and its temperature dependence should provide the reaction enthalpy. One has to be aware, though, of various complications that can affect the accuracy of such estimation. Absorption profile can change with temperature, close lying bands may overlap: in particular, a higher energy band corresponding to the form absorbing at lower energies may be hidden under the origin of the absorption of the other form. The enthalpy itself may also change with temperature. In order to determine the reaction enthalpy as accurately as possible, we measured the absorption in a wide temperature range (93 – 373 K) for various solvents or solvent mixtures (3-methylpentane, dodecane, and EPA (2:2:5 mixture of ethyl ether/isopentane/ethanol)). An example of the temperature dependence of **HPc** absorption is shown in Figure 3, where we also show the corresponding van't Hoff plots. The values of ΔH = 1.12 and 1.31 kcal/mol were obtained using either absorption maxima or the areas of the 622/612 nm bands. These values are in very good agreement with the results of DFT simulations. Similar values of the reaction enthalpy were obtained for other solvents and temperature ranges, with somewhat smaller values (about 1 kcal/mol or less) for the samples measured in the low temperature ranges (93-293 K). Practically the same values were also obtained by spectrofluorimetric measurements, as discussed below in the section devoted to photophysics.
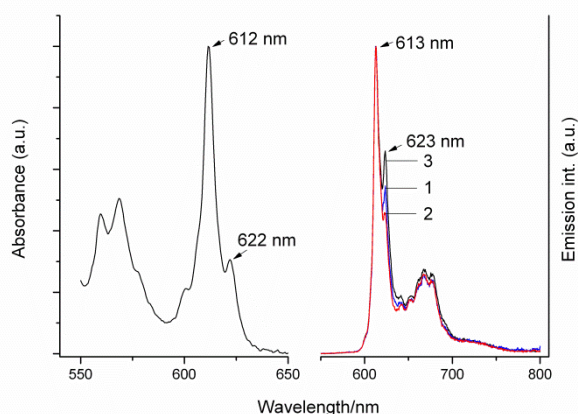
Figure 2. Absorption (left) and emission (right) of **HPc** solution in *n*-hexane at 293 K. Fluorescence curves are shown for three excitation wavelengths: 568 (1, blue), 532 (2, red), and 394 nm (3, black).
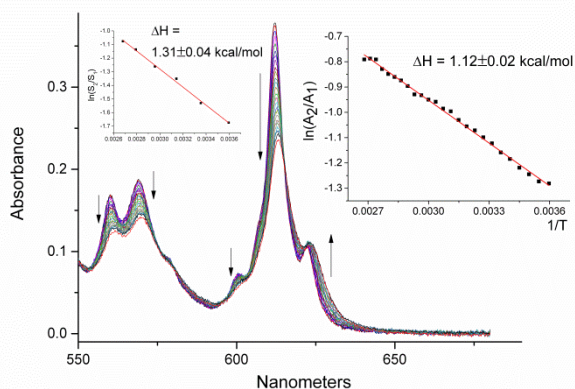
Figure 3. Absorption spectra of **HPc** in dodecane recorded between 298 and 373 K at temperature intervals of 4 K. The arrows indicate spectral changes observed upon heating. Insert, the van't Hoff plots, where A_1/A_2 and S_1/S_2 denote the absorbances at maximum and the areas of the peaks centered at 622 and 612 nm, respectively.

TD-DFT calculations predict the $S_1 \leftarrow S_0$ absorption in *trans1* and *trans2* to occur at 538 and 547 nm, respectively. Even though the theoretical transition energies are overestimated, the ordering and the energy separation are in perfect agreement with experiment. We therefore safely assign the lowest energy form of **HPc** to the *trans1* tautomer. Using the experimentally observed shift in the (0-0) transition energies of the two tautomers and the value of $\Delta H = 1.2$ kcal/mol, one obtains $\Delta H = 0.45$ kcal/mol for the lowest excited singlet state. Thus, the energy ordering is preserved, but the two forms get nearly isoenergetic.
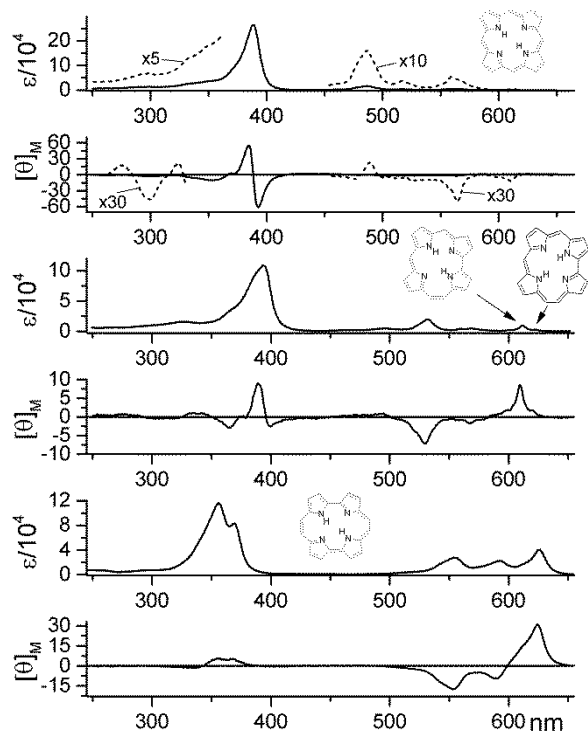
The finding that parent hemiporphycene and its octaethyl derivative behave very similarly with respect to tautomerism is different from what has been observed for porphycene. Alkyl substitution in porphycene may lead to the appearance of *cis* species,[26] whereas they are not detected in solutions of the parent compound. At first, one could attribute this difference between the two isomers to a larger rigidity of **HPc** skeleton. It is well known that the dimensions of the inner cavity in porphycene are very sensitive to substitution. The distance between the H-bonded nitrogen atoms increases from 263 pm in the parent **Pc**[2] to 280 pm in the octaethyl derivative.[27] On the contrary, the separation between the non-H-bonded nitrogen atoms decreases from 289 to 273 pm, so that the longer N-N distance in parent **Pc** becomes shorter, and *vice versa*, upon octaethyl substitution.

Geometry optimizations performed for *trans1* and *trans2* tautomers of **HPc** yield practically the same cavity dimensions in both forms. For **OEHPc** the calculations predict the N21N22 and N23N24 distance to increase by 9 and 15 pm, respectively. The N21N24 and N22N23 distances decrease by 5 and 8 pm. While somewhat smaller than in porphycene, these changes are not dramatically different. We therefore conclude that not only the steric, but also electronic effects, more important in porphycene, are responsible for different responses to alkyl substitution in the two isomers. This is confirmed by comparison of the changes in the S_0-S_1 absorption caused by alkylation: 27 nm for **Pc** vs 20 nm for **HPc**. Yet another argument is provided by comparison of proton chemical shifts caused by octuple alkylation: an upfield shift of 1.8 is observed for **HPc**, whereas the corresponding value for **Pc** is 2.50.

The observation that electronic factors, rather than steric ones, are crucial for the H-bond strength seems to be general for porphyrin isomers. We recently reported a similar behavior for corrphycene and its alkylated derivatives.[28]

Spectroscopy. Absorption and magnetic circular dichroism (MCD) spectra of **Pr**, **HPc**, **and Pc** are presented in Figure 4. All three compounds reveal the pattern of electronic transitions characteristics for porphyrinoids: low energy, weak Q bands are followed in the blue region by stronger absorption (Soret bands). However, large differences in intensities are observed between the isomers. The Soret transitions are much stronger in **Pr** than in the other two compounds, where they are of comparable intensity. On the contrary, the absorption in the Q region is the weakest in porphyrin and strongest in porphycene. Such intensity pattern is predicted by simple Gouterman[29] and perimeter[30] models, which describe the Q and Soret transitions in terms of interactions between single electron configurations involving two highest occupied and two lowest unoccupied molecular orbitals (HOMO and LUMO, respectively). According to the perimeter model, the ratio of dipole strengths (and thus, absorption intensities) for transitions in the Q vs Soret regions should scale as $|\Delta HOMO^2 - \Delta LUMO^2|$, where $\Delta HOMO$ and $\Delta LUMO$ denote the energy splitting in the pairs of occupied and unoccupied frontier orbitals.[31] In agreement with this prediction, the calculated values of $\Delta HOMO$ and $\Delta LUMO$ are 0.12 and 0.01 eV for **Pr**, 0.03 and 0.55 eV for **HPc**, and 0.06 and 1.28 eV for **Pc** (Figure 5).
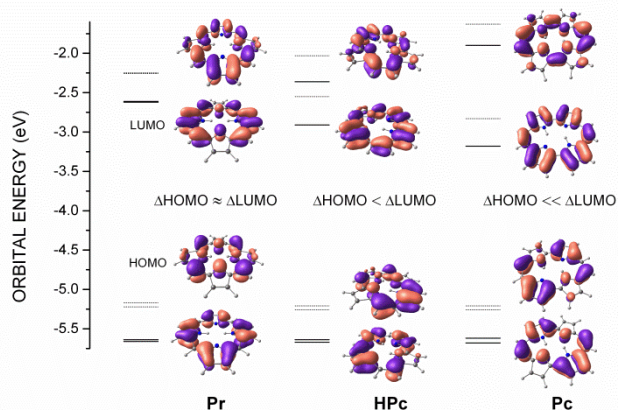
The sign and value of ΔHOMO - ΔLUMO is crucial for the prediction of MCD signs and intensities. When the orbital splittings are very different, the sign of ΔHOMO - ΔLUMO determines the MCD pattern of the four lowest transitions described by the perimeter model. This pattern is difficult to change by such perturbations as substitution. Porphycene, with ΔHOMO << ΔLUMO is a typical example of such a "hard" chromophore. On the other hand, when the orbital splittings are similar, even a weak perturbation may lead to a change in the sign of ΔHOMO – ΔLUMO and, in consequence, to a different MCD pattern. Porphyrin, with small and similar values of ΔHOMO and ΔLUMO represents this class of "soft" chromophores.

Both theory and experiment show that hemiporphycene should be described as a hard chromophore, although the value of |ΔHOMO – ΔLUMO| is definitely smaller than in porphycene. Interestingly, absorption and MCD spectra of **HPc** and its octaethyl derivative are very similar,[32] which is not the case for **Pr** and **Pc**. The reason is a very similar pattern of frontier orbitals ordering in the parent **HPc** and its octaethyl derivative (Figure 5). One should note, though, that alkyl substitution leads to a shift in orbital energies, which results in different redox potentials. This effect will be discussed below.

The analysis of the MCD spectra of **HPc** reveals a presence of a weak electronic transition located around 490 nm, between the Q and Soret bands. Regarding the latter, the MCD curves demonstrate that at least three different electronic transitions are present in the Soret region. Therefore, the analysis based on four orbital model may not be very accurate in the region of the Soret bands.

Comparison of the absorption and MCD spectra of the three isomers (Figure 4) clearly shows much larger variations in the case of MCD. A spectacular difference between **Pr** and **Pc** is the reversal of the intensity ratio of the signals from Q and Soret transitions observed in the MCD: very weak MCD signal is observed for **Pr** in the Q region, whereas the intensity is quite strong for Soret transitions. The opposite occurs in **Pc**, where the MCD curve exhibits the strongest intensity in the low energy range. Hemiporphycene behaves in an intermediate fashion, revealing similar intensities in the two regions. Exactly such MCD patterns are predicted using the perimeter model; a detailed discussion has already been provided for porphycenes.[31] In short, the MCD intensity results from interplay between two magnetic moment terms, μ^+ and μ^-. Their relative contributions depend on the degree of perturbation of an ideal perimeter that leads to a given chromophore. All porphyrin isomers are obtained by the same type of perturbations, but in each case they act at different positions of the perimeter. As a result, the orbital energy patterns are different, as shown in Figure 5. For porphyrin, a soft chromophore (ΔHOMO ≈ ΔLUMO), μ^+ contribution vanishes; for such case, the expected sign sequence of the Faraday B terms for the four lowest excited electronic states is +,+,+,-, with the two lowest ones having very weak intensity. For ΔHOMO < ΔLUMO, the situation is different. The S_1 and S_2 (Q bands) should always exhibit a -,+ sequence. With the growing inequality of orbital splittings, the B term of the first Q transition should become more negative, and that of the

Figure 4. Absorption and MCD spectra at 293K. Top, **Pr** in acetonitrile, middle, **HPc** in *n*-hexane, bottom, **Pc** in acetonitrile.

Figure 5. Energies and shapes of frontier orbitals, calculated at the B3LYP/6-311++G(d,p) level. Dashed lines show the energies calculated for octaethyl derivatives.

second transition, more positive (we recall that a negative *B* term corresponds to a positive MCD signal and *vice versa*). This is exactly what is observed and calculated for **HPc** and **Pc** (Figures 4 and 5), the latter being a stronger negative-hard chromophore. In the region of Soret transitions, the situation is more complicated: one can expect a change from the -,+ to the +,- sequence of *B* terms when the ratio of dipole strengths D(Q)/D(Soret) exceeds a certain value; this change should first happen for the lower energy Soret transition. Indeed, such behavior is observed for **Pc**, but not for **HPc**, which exhibits in the Soret region the -,+ sequence, the same as in the Q region and typical for a moderately strong negative-hard chromophore.

Photophysics. **HPc** reveals fairly strong fluorescence, with the quantum yield intermediate between those of **Pr** and **Pc**. The differences are due to the radiative constants, increasing in the order: **Pr** < **HPc** < **Pc**. Such sequence is readily predicted by the perimeter model as the consequence of the increasing value of ΔHOMO + ΔLUMO.[31] The radiationless deactivation constants are similar in the three isomers, as demonstrated by similar fluorescence decay times (Table 2).

Table 2. Photophysical parameters of **HPc** (293 K) compared with the corresponding values in **Pr** and **Pc**.

Head 1[a]	Fluorescence quantum yield	Fluorescence decay time [ns]	k_r [10^7s^{-1}]	$\sum k_{nr}$ [10^7s^{-1}]
Pr	0.043 [a]	9.6 [a]	0.45	9.97
	0.054 [b]	15.3 [b]	0.35	6.25
HPc *trans1*	0.12	7.7	1.6	11.4
HPc *trans2* [c]	0.18	8.9	2.0	9.2
Pc	0.36 [d]	10.2 [d]	3.5	6.3

[a] Ref. 40. [b] ref. 41. [c] in *n*-hexane. [d] ref. 42.

As already mentioned, the fluorescence spectra reveal the presence of two *trans* tautomers, with their 0-0 bands separated by 10 nm, similar as in absorption. The intensity ratio of the two emissions strongly depends on the excitation wavelength (Figure 2). Correspondingly, the excitation spectra are different when monitored in different spectral regions (Figure 6). This indicates lack of excited state equilibrium between the two tautomeric forms, a situation very different from that in porphycene, where the time required for *trans-trans* conversion (single picoseconds) is about a thousand times shorter than the S$_1$ lifetime.[33] **HPc** behaves in this respect similarly to **Pr**, where no tautomerization occurs in S$_1$.[34]

Both emissions in **HPc** decay with similar lifetimes, indicating similar values of radiationless deactivation rates. For selective excitation of *trans2* in *n*-hexane at 293, monoexponential decay was observed, with the S$_1$ lifetime of 8.9±0.2 ns. For excitations into regions where both tautomers absorb, we monitored the

decays in several spectral channels, each of 12.5 nm width. Again, the kinetic profiles were monoexponential, but a characteristic pattern was observed: For the channels where fluorescence was dominated by the *trans1* form, the decay time was definitively shorter (7.7-8.0 ns). A similar behaviour was exhibited by **HPc** dissolved in dodecane, but now the lifetimes were definitely longer (Figure S22), changing between 9 and 12 ns in the regions dominated by *trans1* and *trans2*, respectively. A similar pattern was observed at higher temperatures, but with the decay time values now spanning a narrower range.
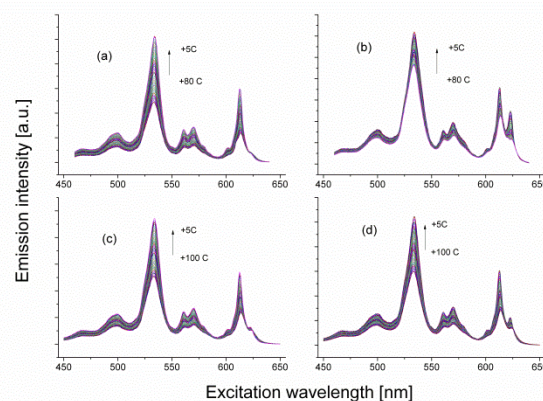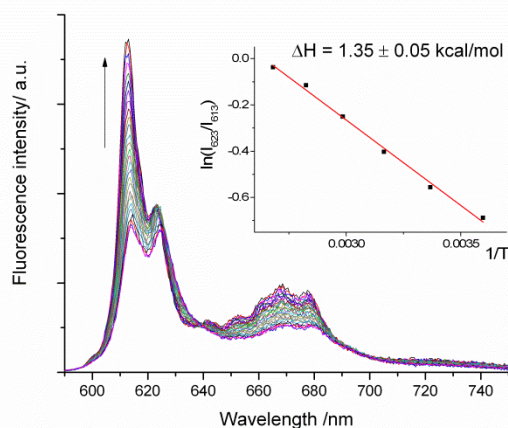

Figure 6. Fluorescence excitation spectra of **HPc** in dodecane recorded between 298 and 353(373) K at temperature intervals of 4 K. The emission was monitored at 609 (a), 620 (b), 660 (c), and 680 nm (d). The arrows indicate spectral changes observed upon cooling.

The kinetic data suggested that the fluorescence quantum yields of *trans1* and *trans2* may not be the same, indicating the lower value for the former. In addition, longer lifetimes in dodecane compared with *n*-hexane could be due to different viscosities. These predictions were confirmed by measuring the fluorescence quantum yield as a function of excitation wavelength in three different solvents: *n*-hexane, dodecane, and tetradecane. In all these solvents, the same pattern of wavelength dependence of total quantum yield was observed, with the minimum for excitation at the absorption maximum of *trans1* (Figure S23). Moreover, for each excitation wavelength the quantum yield increases with solvent viscosity. This suggests a mechanism of S$_1$ deactivation that includes large amplitude motion, a model previously proposed to explain the radiationless transitions in porphycenes.[25] In this model, the structure responsible for radiationless deactivation is the *cis* form in which the two inner protons get so close to each other that the molecule becomes nonplanar due to twisting of the pyrrole subunits in opposite directions. For **HPc**, such form corresponds most probably to *cis4*. In order to determine whether such form is more readily accessible from *trans1* or *trans2*, we compared the S$_1$ optimized geometries of the two forms. The distance between the proton that has to move and the target nitrogen atom is 251 pm in *trans1* and 275 pm in *trans2*. Since the *trans1-cis4* conversion involves a smaller proton displacement than the *trans2-cis4* tautomerization, faster

deactivation, and a smaller quantum yield can be expected for *trans1*, exactly as observed. This effect is sufficiently strong to overcome another S_1 depopulation channel that should otherwise make *trans2* less emissive than *trans1*. This channel is the *trans2-trans1* conversion. Closer examination of the excitation spectrum monitored in the region where only the *trans1* form emits (609 nm, Figure 6a) suggests that a small fraction of excited *trans1* can be produced via excitation of *trans2*. This was checked by recording fluorescence as a function of temperature for three wavelengths for which the absorption may be assumed to be exclusively due to *trans2*. Using the ratio of *trans1* and *trans2* emission intensities (measured at 613-615 and 623-625 nm, respectively) (Figure S24), it was estimated that at room temperature and below, at most 10% of excited *trans2* is converted to *trans1*, but at 373 K this fraction reaches about 50%. The rate of *trans2→trans1* excited state reaction at 293 K can be estimated from the values of fluorescence decay time (ca. 10 ns) and the tautomerization yield. Assuming 10% for the latter leads to the reaction rate of 10^7 s^{-1}, four orders of magnitude slower than that determined for S_1 tautomerization in porphycene.[33]

The emission lifetimes measured at 373 K for *trans1* and *trans2* were, while still somewhat different, closer to each other than at room temperature, showing that the excited state tautomerization process is approaching the equilibrium.

The lack of excited state interconversion and the same response of both emissions to temperature are the conditions for an independent determination of the ground state *trans1 - trans2* reaction enthalpy using spectrofluorimetric methods. Even though the first condition is not strictly obeyed, especially at elevated temperatures, we checked whether this methodology can still be applied to **HPc**. Fluorescence has been recorded at different temperatures using the excitation wavelengths for which the absorption remained constant over the whole temperature range. The enthalpy value was extracted from the ratio of fluorescence maxima corresponding to both forms (Figure 7). Since the method is reliable only when the absorption coefficients of both forms do not change with temperature, three different wavelengths have been used: For excitation at 614.5 and 574 nm, the obtained ΔH values were practically the same as those determined using absorption: 1.35 and 1.31 kcal/mol, respectively. However, for excitation at 541.5 nm the obtained ΔH value was unrealistically low (0.4 kcal.mol); apparently the assumption of the absorption coefficients of both *trans1* and *trans2* forms being temperature-independent does not hold in this case.

Figure 7. Temperature dependence of fluorescence of **HPc** in dodecane for 614 nm excitation. The spectra were recorded between 278 and 373 K every 4 K. The arrow shows the changes observed upon cooling. Insert, van't Hoff plot based on the ratio of fluorescence maxima at 613 and 623 nm.
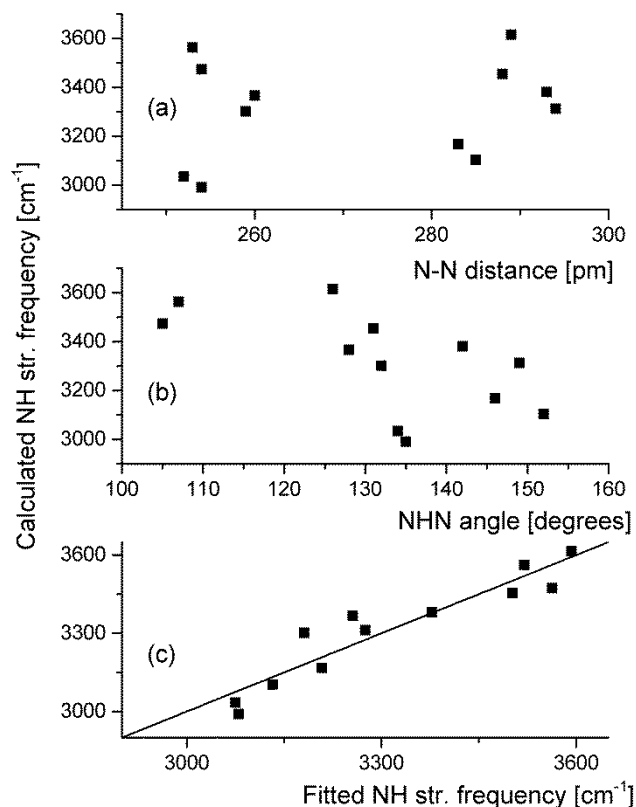
Vibrational structure. IR and Raman spectra have been measured for **HPc** and compared with theoretical predictions obtained for all six possible tautomeric forms (Figures S25 and S26). The comparison leaves no doubt that the dominant form is the *trans1* tautomer. The determination of the NH stretching frequencies was not straightforward, as the corresponding bands overlap with those caused by CH stretching. This is demonstrated by very similar positions and intensities of IR bands recorded for **Pc** and **HPc** (Figure 8a). This analogy allows to assign the bands observed in **HPc** at 3024, 3086, and 3105 cm^{-1} to CH stretches. A broad underlying absorption with peaks around 3040 and 3140 cm^{-1} is attributed to the NH stretches. Such assignment is confirmed by the disappearance of these bands upon deuteration of the inner nitrogen atoms (Figure 8b). The location of the NH stretching bands, intermediate between those observed in **Pr** (3320 cm^{-1})[35] and **Pc** (< 3000 cm^{-1})[36] demonstrates that the hydrogen bonds in **HPc** are definitely weaker than in **Pc**, but stronger than in **Pr**. Such conclusion is not surprising, given the geometries of the three isomers. What is rather unusual though, is the theoretical prediction (Table 1) that for the *trans1* tautomer the calculated lower frequency NH stretch (and thus, stronger of the two NH···N bonds in **HPc**) corresponds to a longer N···N distance. This effect is caused by very different NHN angles, 128 and 149 degrees, the smaller one overcoming the effect due to smaller distance (260 vs 294 pm). In the *trans2* form, the calculated distances remain almost the same (259 and 293 pm), but the angles become similar (132 and 142 degrees). As a result, now the shorter H-bond is predicted to be stronger, judging from the value of the NH stretching frequency.
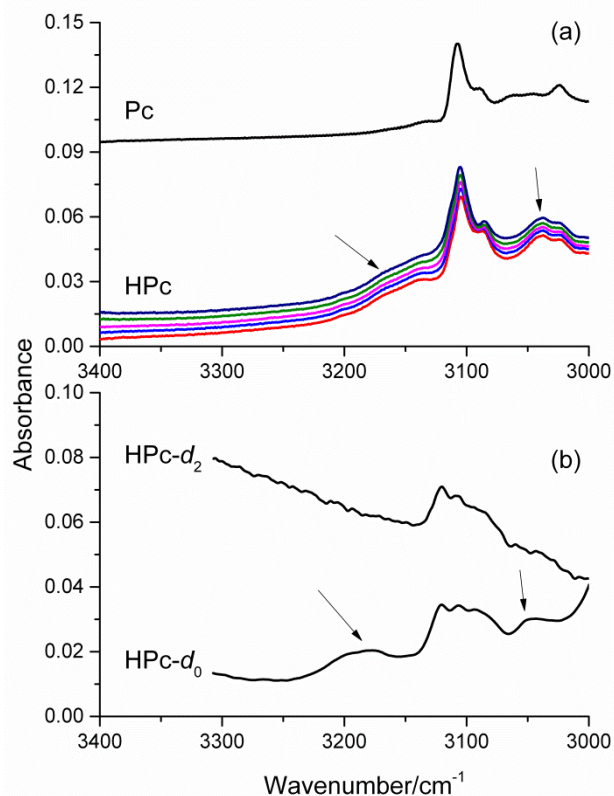
Figure 8. Top, portions of IR spectra recorded for solutions of **Pc** and **HPc** in carbon disulfide solutions (293 K for **Pc**, 213-233 K in steps of 5 K for **HPc**). Bottom, spectra of **HPc** and its doubly deuterated isotopologue recorded at 293 K in KBr pellets. The arrows indicate the positions of NH stretching bands.

Figure 9. Plots of calculated NH stretching frequencies (*cf.* Table1) vs: (a) N-N distances; (b) NHN angles. (c) Correlation between the calculated frequencies and the values obtained by multiple linear regression, using the relation: $\nu_{NH} = a_0 + a_1 d_{NN} + a_2 \alpha_{NHN}$.

We analyzed the distance/angle effects for all twelve H-bonds in six optimized structures of **HPc**, by plotting the calculated NH stretching frequency (ν_{NH}) vs these structural parameters. No correlation was obtained for separate plots of ν_{NH} vs the distance or the angle. However, a nice correlation has been observed when both the distance and the angle were simultaneously taken into account (Figure 9). We tried the simplest possible form of multiple regression, using the relation: $\nu_{NH} = a_0 + a_1 d_{NN} + a_2 \alpha_{NHN}$. It may be transformed into a more physically relevant form: $\nu_{NH} = \nu_0 + a_1(d_{NN}-d_0) + a_2(180-\alpha_{NHN})$, where ν_0 and d_0 denote the frequency and N-N distance of an ideal, "strongest possible", linear ($\alpha = 180°$) H-bond. Satisfactory fits were observed for ν_0 varying between 2300-2600 cm^{-1}, and d_0 around 250 pm. We note that these values are close to those postulated for porphycenes, which form exceptionally strong intramolecular hydrogen bonds.[36,37]

The detailed analysis of the vibrational structure of **HPc** will be a subject of a separate work. We note two factors that make such investigations more complex in comparison with **Pr** and **Pc**. The first is the presence of two tautomers in **HPc**. The second is the lower symmetry (in particular, loss of the centre of inversion results in the lack of mutual exclusion principle, valid for the other two isomers).

Redox properties. The first two averaged reduction potentials of **HPc** are -1.02 V and -1.41 V, respectively. **Pc** is much easier to reduce, with the corresponding values of -0.73 and -1.07.[38] Only one irreversible oxidation step was observed for **HPc** at +1.13V. Similar behavior was found for **Pc**, where the irreversible oxidation occurred at about +1 V.[38,39] The differences in the reduction and similar oxidation potentials are readily explained by inspection of the calculated orbital energy values (Figure 5). Also the shifts in the redox potentials towards lower values observed in the ethyl-substituted derivatives are in perfect agreement with theoretical predictions. Finally, nice correlation exists between the difference between the first

oxidation and reduction potential and the calculated HOMO-LUMO energy gap (Figure S27).

Summary and conclusions

Successful, rational synthesis of parent, unsubstituted hemiporphycene, followed by extensive structural, spectral, photophysical, and electrochemical studies allowed a detailed comparison with porphyrin and porphycene. In many respects, the properties of hemiporphycene justify its name. The values of various parameters that characterize the structure and properties, such as N-N distances, orbital energy splittings, absorption coefficients, MCD parameters, NH stretching frequencies, fluorescence quantum yields, tautomerization rate, and redox potentials lie in-between those determined for **Pr** and **Pc**. The knowledge of the electronic structure allows making predictions about the behavior of substituted hemiporphycenes. For instance, the negative-hard character of the hemiporphycene chromophore (ΔHOMO < ΔLUMO) implies that, contrary to porphyrin, the ratio of absorption intensities in the Q and Soret regions will not be changing dramatically after substitution and/or protonation/deprotonation. Also the MCD pattern of differently substituted hemiporphycenes should remain the same. In fact, this prediction has been already confirmed by MCD studies of neutral and ionic forms of **OEHPc**.[32]

The areas of fundamental research where hemiporphycenes look extremely promising include intramolecular hydrogen bond, tautomerism, and proton transfer, both in the ground and electronically excited states. Low symmetry of **HPc** results in the existence of two tautomers being close in energy, each of them characterized by two different, unsymmetrical hydrogen bonds. Further studies of such systems should allow a better understanding of the roles the electronic and geometrical factors play in hydrogen bond structure and reactivity. Of particular interest is the finding that predicting relative strength of H-bonds based on the NMR shifts and NH stretching vibrations may give opposite results. In order to investigate such unusual cases in more detail, we plan to extend the hemiporphycene family by derivatives in which one of the inner nitrogens will be replaced by the oxygen atom.

The present work has established the thermodynamic aspects of tautomerization in **HPc**. Further investigations are planned, regarding the kinetics. Since the populations of the two *trans* tautomers are uneven already at room temperature, studies by variable temperature NMR are not possible. We currently investigate the kinetics using pump-probe transient absorption techniques.

The difference in fluorescence quantum yields in the two *trans* tautomers of **HPc** can be explained by a model that proposes that the nonradiative S_1 deactivation process in **HPc** involves *trans-cis* tautomerization, followed by distortion from planarity. It is tempting to suggest that such model may be general for different porphyrin isomers, since it was used previously to explain the photophysics of porphycenes.[25]

Finally, we would like to make a general comment on the subject of determination of thermodynamic parameters from spectral measurements. Our value of ground state enthalpy difference between the two forms of **HPc** was estimated independently from absorption and emission. Both methods yielded practically the same value, even though the conditions required for spectrofluorimetric measurements were not strictly met. It may be that some cancellation of errors (due to e.g., change in absorption coefficients, absorption/emission band location and shape) has led to similar values obtained using the two procedures. Moreover, the van't Hoff plots were nicely linear, yielding, for each fit, large correlation coefficients and very small errors. This may create a false impression about the high accuracy of such spectral titrations. Still we believe that the unquestionably accurate results can only be obtained with a technique that allows to observe **separate** signals from each species. In this context, we are planning to investigate the tautomeric equilibria in **HPc** using Raman and IR spectroscopies.

[1]   *Handbook of Porphyrin Science: with Applications to Chemistry, Physics, Materials Science, Engineering, Biology and Medicine*, World Scientific, Singapore, **2010-2012**.

[2]   E. Vogel, M. Köcher, H. Schmickler, J. Lex, *Angew. Chem. Int. Ed.* **1986**, *25*, 257-259.

[3]   J. Waluk, J. Michl, *J. Org. Chem.* **1991**, *56*, 2729-2735.

[4]   E. Vogel, M. Bröring, S. J. Weghorn, P. Scholz, R. Deponte, J. Lex, H. Schmickler, K. Schaffner, S. E. Braslavsky, M. Müller, S. Pörting, C. J. Fowler, J. L. Sessler, *Angew. Chem. Int. Ed.* **1997**, *36*, 1651-1654.

[5]   H. J. Callot, B. Metz, T. Tschamber, *New J. Chem.* **1995**, *19*, 155-159.

[6]   J. L. Sessler, E. A. Brucker, S. J. Weghorn, M. Kisters, M. Schäfer, J. Lex, E. Vogel, *Angew. Chem. Int. Ed.* **1994**, *33*, 2308-2312.

[7]   M. A. Aukauloo, R. Guilard, *New J. Chem.* **1994**, *18*, 1205-1207.

[8]   E. Vogel, P. Scholz, R. Demuth, C. Erben, M. Bröring, H. Schmickler, J. Lex, G. Hohlneicher, D. Bremm, Y. D. Wu, *Angew. Chem. Int. Ed.* **1999**, *38*, 2919-2923.

[9]   E. Vogel, M. Bröring, C. Erben, R. Demuth, J. Lex, M. Nendel, K. N. Houk, *Angew. Chem. Int. Ed.* **1997**, *36*, 353-357.

[10] T. Morimoto, S. Taniguchi, A. Osuka, H. Furuta, *Eur. J. Org. Chem.* **2005**, *2005*, 3887-3890.

[11] P. J. Chmielewski, L. Latos-Grażyński, K. Rachlewicz, T. Glowiak, *Angew. Chem. Int. Ed.* **1994**, *33*, 779-781.

[12] H. Furuta, T. Asano, T. Ogawa, *J. Am. Chem. Soc.* **1994**, *116*, 767-768.

[13] J. P. Gisselbrecht, M. Gross, E. Vogel, P. Scholz, M. Bröring, J. L. Sessler, *J. Electroanal. Chem.* **2001**, *507*, 244-249.

[14] C. J. Fowler, J. L. Sessler, V. M. Lynch, J. Waluk, A. Gebauer, J. Lex, A. Heger, F. Zuniga-y-Rivero, E. Vogel, *Chem.-Eur. J.* **2002**, *8*, 3485-3496.

[15]   S. Neya, K. Imai, H. Hori, H. Ishikawa, K. Ishimori, D. Okuno, S. Nagatomo, T. Hoshino, M. Hata, N. Funasaki, *Inorg. Chem.* **2003**, *42*, 1456-1461.

[16]   D. Maeda, H. Shimakoshi, M. Abe, Y. Hisaeda, *Inorg. Chem.* **2009**, *48*, 9853-9860.

[17]   R. Paolesse, S. Nardis, M. Stefanelli, F. R. Fronczek, M. G. H. Vicente, *Angew. Chem. Int. Ed.* **2005**, *44*, 3047-3050.

[18]   Y. Y. Fang, F. Mandoj, S. Nardis, G. Pomarico, M. Stefanelli, D. O. Cicero, S. Lentini, A. Vecchi, Y. Cui, L. H. Zeng, K. M. Kadish, R. Paolesse, *Inorg. Chem.* **2014**, *53*, 7404-7415.

[19]   S. Neya, J. S. Quan, T. Hoshino, M. Hata, N. Funasaki, *Tetrahedron Lett.* **2004**, *45*, 8629-8630.

[20]   T. M. Krygowski, M. K. Cyrański, *Chem. Rev.* **2001**, *101*, 1385-1419.

[21]   P. von Ragué Schleyer, C. Maerker, A. Dransfeld, H. Jiao, N. J. R. v. E. Hommes, *J. Am. Chem. Soc.* **1996**, *118*, 6317-6318.

[22]   D. Bremm, G. Hohlneicher, *J. Mol. Struct.* **1999**, *480-481*, 591-594.

[23]   M. Bröring, PhD thesis, University of Cologne, **1996.**

[24]   J. Waluk in *Structure, spectroscopy, photophysics, and tautomerism of free-base porphycenes and other porphyrin isomers Vol. 7* (Ed. K. Smith, Kadish, K., Guilard, R.), World Scientific, Singapore, **2010**, pp.359.

[25]   A. Sobolewski, M. Gil, J. Dobkowski, J. Waluk, *J. Phys. Chem. A* **2009**, *113*, 7714-7716.

[26]   M. Gil, J. Dobkowski, G. Wiosna-Sałyga, N. Urbańska, P. Fita, C. Radzewicz, M. Pietraszkiewicz, P. Borowicz, D. Marks, M. Glasbeek, J. Waluk, *J. Am. Chem. Soc.* **2010**, *132*, 13472-13485.

[27]   E. Vogel, P. Koch, X. L. Hou, J. Lex, M. Lausmann, M. Kisters, M. A. Aukauloo, P. Richard, R. Guilard, *Angew. Chem. Int. Ed.* **1993**, *32*, 1600-1604.

[28]   A. Gorski, B. Leśniewska, G. Orzanowska, J. Waluk, *J. Porphyrins Phthalocyanines* **2016**, *20*, in press.

[29]   M. Gouterman, *J. Mol. Spectrosc.* **1961**, *6*, 138-163.

[30]   J. Michl, *Tetrahedron* **1984**, *40*, 3845-3934.

[31]   J. Waluk, M. Müller, P. Swiderek, M. Köcher, E. Vogel, G. Hohlneicher, J. Michl, *J. Am. Chem. Soc.* **1991**, *113*, 5511-5527.

[32]   A. Gorski, E. Vogel, J. L. Sessler, J. Waluk, *Chem. Phys.* **2002**, *282*, 37-49.

[33]   P. Fita, N. Urbańska, C. Radzewicz, J. Waluk, *Chem.- Eur. J.* **2009**, *15*, 4851-4856.

[34]   S. Gawinkowski, G. Orzanowska, K. Izdebska, M. O. Senge, J. Waluk, *Chem.- Eur. J.* **2011**, *17*, 10039-10049.

[35]   J. G. Radziszewski, J. Waluk, J. Michl, *Chem. Phys.* **1989**, *136*, 165-180.

[36]   S. Gawinkowski, Ł. Walewski, A. Vdovin, A. Slenczka, S. Rols, M. R. Johnson, B. Lesyng, J. Waluk, *Phys.Chem.Chem.Phys.* **2012**, *14*, 5489-5503.

[37]   P. Ciąćka, P. Fita, A. Listkowski, M. Kijak, S. Nonell, D. Kuzuhara, H. Yamada, C. Radzewicz, J. Waluk, *J. Phys. Chem. B* **2015**, *119*, 2292-2301.

[38]   J. P. Gisselbrecht, M. Gross, M. Kocher, M. Lausmann, E. Vogel, *J. Am. Chem. Soc.* **1990**, *112*, 8618-8620.

[39]   C. Bernard, J. P. Gisselbrecht, M. Gross, E. Vogel, M. Lausmann, *Inorg. Chem.* **1994**, *33*, 2393-2401.

[40]   A. T. Gradyushko, M. P. Tsvirko, *Opt. Spectrosc. (Russ.)* **1971**, *31*, 548-556.

[41]   O. Ohno, Y. Kaizu, H. Kobayashi, *J. Chem. Phys.* **1985**, *82*, 1779-1787.

[42]   P. F. Aramendia, R. W. Redmond, S. Nonell, W. Schuster, S. E. Braslavsky, K. Schaffner, E. Vogel, *Photochem. Photobiol.* **1986**, *44*, 555-559.

Entry for the Table of Contents

Layout 1:

FULL PAPER

Rational synthesis of parent, "bare" hemiporphycene, a constitutional isomers of porphyrin followed by extensive structural, spectral, photophysical, and electrochemical studies allowed a detailed comparison with porphyrin and another isomer, porphycene.
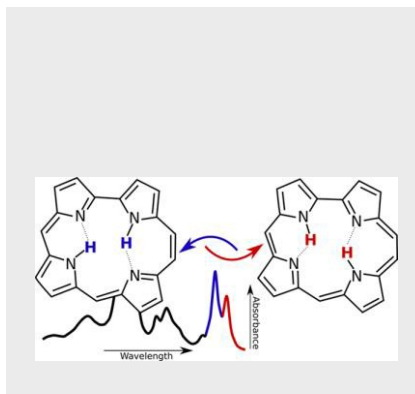
Jakub Ostapko, Krzysztof Nawara, Michał Kijak, Joanna Buczyńska, Barbara Leśniewska, Mariusz Pietrzak, Grażyna Orzanowska, Jacek Waluk*]

Page No. – Page No.

Parent, unsubstituted hemiporphycene: synthesis and properties